

Giant planar Hall effect in topological metals

A. A. Burkov

Department of Physics and Astronomy, University of Waterloo, Waterloo, Ontario, Canada N2L 3G1

(Received 21 April 2017; published 10 July 2017)

Much excitement has been generated recently by the experimental observation of the chiral anomaly in condensed matter physics. This manifests as strong negative longitudinal magnetoresistance and has so far been clearly observed in Na_3Bi , ZrTe_5 , and GdPtBi . In this Rapid Communication, we point out that the chiral anomaly must lead to another effect in topological metals, the giant planar Hall effect (GPHE), which is the appearance of a large transverse voltage when the in-plane magnetic field is not aligned with the current. Moreover, we demonstrate that the GPHE is closely related to the angular narrowing of the negative longitudinal magnetoresistance signal, observed experimentally.

DOI: [10.1103/PhysRevB.96.041110](https://doi.org/10.1103/PhysRevB.96.041110)

The recent theoretical [1–8] and experimental [9–14] discovery of Dirac and Weyl semimetals has extended the notions of nontrivial electronic structure topology to metals. It has also reinforced the connection that exists between the physics of materials with topologically nontrivial electronic structures and the physics of relativistic fermions. Chiral anomaly, which refers to nonconservation of the chiral charge in the presence of collinear external electric and magnetic fields, is a particularly important example that highlights such a connection. Discovered theoretically by Adler [15] and by Bell and Jackiw [16] in the relativistic particle physics context, it provided the explanation for the observed fast decay of a neutral pion into two photons, naively not allowed by the chiral charge conservation. Very recently, a condensed matter manifestation of the chiral anomaly was finally observed in Dirac semimetals Na_3Bi [17], ZrTe_5 [18], and in a half-Heusler compound GdPtBi [19].

The chiral anomaly manifests in Weyl and Dirac semimetals as a very unusual large negative longitudinal magnetoresistance, quadratic in the applied magnetic field, as predicted theoretically [20–22]. While the existence of the effect, and most of its observed features, are in qualitative agreement with the theory, one puzzling feature has remained unexplained. As was first pointed out in Ref. [17], the observed dependence of the magnetoresistance on the angle θ between the current and the applied magnetic field is against the expectations, drawn from the existing theory. Namely, the theory of Refs. [20–22] naively predicts a $\cos^2\theta$ dependence, due to the quadratic dependence of the chiral anomaly contribution to the conductivity on the magnetic field, but the observed angular dependence appears to be much stronger.

In this Rapid Communication, we both explain the angular narrowing phenomenon and connect it with another effect, the giant planar Hall effect (GPHE). Note that a closely related explanation of the angular narrowing effect has already been proposed by us in Ref. [23], but the connection with the GPHE was not understood there. We argue that the presence of both the negative longitudinal magnetoresistance with a characteristic dependence on the angle between the current and the magnetic field, and the GPHE, may be regarded as a smoking gun signature of the chiral anomaly.

As was argued in Refs. [20–22,24], transport in topological (both Weyl and Dirac) metals is distinguished by the existence

of an extra (nearly) conserved quantity, the chiral charge, which is coupled to the electric charge in the presence of an external magnetic field. The hydrodynamic transport equations for the electric and the chiral charge have the following form [21,22],

$$\begin{aligned}\frac{\partial n}{\partial t} &= D\nabla^2(n + gV) + \Gamma\mathbf{B} \cdot \nabla(n_c + gV_c), \\ \frac{\partial n_c}{\partial t} &= D\nabla^2(n_c + gV_c) - \frac{n_c + gV_c}{\tau_c} + \Gamma\mathbf{B} \cdot \nabla(n + gV).\end{aligned}\quad (1)$$

Here, $-en$ is the electric charge density, and $-en_c$ is the chiral charge density (defined as the difference between the total right-handed and total left-handed charge); D is the diffusion coefficient (we take the diffusion coefficients, corresponding to the electric and the chiral charges to be the same for simplicity, although they may in general be different due to electron-electron interaction effects); g is the density of states at the Fermi energy; $\Gamma = e/2\pi^2g$ is a transport coefficient, which characterizes the chiral anomaly induced coupling between the electric and the chiral charge in the presence of an applied magnetic field \mathbf{B} ; and τ_c is the chiral charge relaxation time, which is taken to be long, reflecting the near conservation of the chiral charge. We will use $\hbar = c = 1$ units throughout this Rapid Communication, except in some of the final results.

The presence of the electrostatic potential V and the “chiral electrostatic potential” V_c (this is a hypothetical external potential that couples antisymmetrically to the right- and left-handed charge) reflects the presence of both diffusion and drift contributions to the electric and chiral currents correspondingly. In equilibrium the two contributions must cancel each other, which, in particular, implies $n_c + gV_c = 0$ in this case. We note that a time-independent spatially uniform V_c will always be present in a noncentrosymmetric topological metal [25].

Let us consider an experimental setup, shown in Fig. 1. We will assume a sample of length L_x in the x direction, attached to current-carrying normal (i.e., nontopological) metallic leads at $x = \pm L_x/2$, and a square (for simplicity) cross section of area L_y^2 . Suppose electric current I is injected and extracted uniformly at the attached leads. We want to find the voltage that

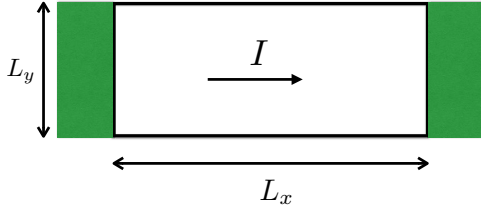


FIG. 1. Schematics of the sample setup. Ordinary metal electrodes (green) are attached along the whole width of the sample cross section and inject current into the sample uniformly. The sample has a square cross section of area L_y^2 and length L_x .

develops in response to this current, or the resistivity tensor of our system.

It is convenient to introduce “electrochemical potentials” $\mu = (n + gV)/g$ and $\mu_c = (n_c + gV_c)/g$. The electric current density is then given by

$$\mathbf{j} = \frac{\sigma}{e} \nabla \mu + eg\Gamma \mu_c \mathbf{B}, \quad (2)$$

where $\sigma = e^2 g D$ is the Drude conductivity. The second term in Eq. (2) expresses the chiral magnetic effect (CME) [26]. Since $\mu_c = 0$ in equilibrium, CME vanishes in equilibrium, as it should [27,28].

We assume that in the steady state the current only flows in the x direction, which means

$$j_x = \frac{I}{L_y^2}, \quad j_y = j_z = 0. \quad (3)$$

We will also assume that the magnetic field is only rotated in the xy plane (the xz plane is identical). This implies that we may take both electrochemical potentials μ and μ_c to be independent of z . Then Eqs. (2) and (3) allow us to express $\nabla \mu$ in terms of the current and the chiral electrochemical potential μ_c as

$$\frac{\partial \mu}{\partial x} = \frac{eI}{\sigma L_y^2} - \frac{\mu_c}{L_a} \cos \theta, \quad \frac{\partial \mu}{\partial y} = -\frac{\mu_c}{L_a} \sin \theta, \quad (4)$$

where $\theta = \arctan(B_y/B_x)$ is the angle between the applied magnetic field and the current and we have introduced a magnetic field related length scale

$$L_a = \frac{D}{\Gamma B}, \quad (5)$$

which will play a crucial role in what follows. Note that this length scale is distinct from the usual magnetic length $\ell_B = 1/\sqrt{eB}$ and appears due to the chiral anomaly (hence the subscript a). $1/L_a$ quantifies the strength of the chiral anomaly induced coupling between the electric and the chiral charge. The existence of this length scale was first pointed out in Ref. [29]. Substituting Eq. (4) into the equation for the chiral electrochemical potential, we obtain

$$\frac{\partial^2 \mu_c}{\partial x^2} + \frac{\partial^2 \mu_c}{\partial y^2} - \frac{\mu_c}{\lambda^2} = -\frac{eI \cos \theta}{\sigma L_a L_y^2}, \quad (6)$$

where

$$\lambda^2 = \frac{L_a^2 L_c^2}{L_a^2 + L_c^2}, \quad (7)$$

and we have introduced another important length scale $L_c = \sqrt{D\tau_c}$, which has the meaning of the chiral charge diffusion length. Transport effects due to the chiral anomaly may be expected to be significant only when L_c is a macroscopic length scale, i.e., when the chiral charge is a nearly conserved quantity. More specifically, as will be shown below, the parameter that determines the strength of the chiral anomaly induced magnetotransport effects in topological metals is the ratio of the two length scales L_c/L_a .

We may further simplify Eq. (6) by noticing that the condition of no charge current in the y direction, expressed by the second of Eqs. (4), may always be satisfied by taking μ_c to be independent of y , which then implies uniform gradient of the electrochemical potential μ in the y direction. Equation (6) then simplifies to

$$\frac{d^2 \mu_c}{dx^2} - \frac{\mu_c}{\lambda^2} = -\frac{eI \cos \theta}{\sigma L_a L_y^2}. \quad (8)$$

Equation (8) needs to be solved with the appropriate boundary conditions. These are naturally not universal and depend on the details of the experimental setup being modeled. We will assume that the sample is attached to uniform current carrying leads across the whole width of the sample cross section, and the lead material is a normal nontopological metal. In this case, chiral charge must rapidly relax upon entering the normal leads and the most appropriate boundary condition is thus of the Dirichlet type,

$$\mu_c(x = \pm L_x/2) = 0. \quad (9)$$

We note, however, that the boundary conditions do not affect the final results at all for large sample sizes $L_x \gg L_a, L_c$ (the scale dependence of transport coefficients is, however, interesting in its own right in this case and may be observable due to the large size of L_c [29]).

Solving Eq. (8) with the above boundary conditions, we obtain

$$\mu_c(x) = \frac{eI \lambda^2 \cos \theta}{\sigma L_a L_y^2} \left[1 - \frac{\cosh(x/\lambda)}{\cosh(L_x/2\lambda)} \right]. \quad (10)$$

Substituting Eq. (10) into Eq. (4), we may now calculate the voltage drops that develop across the sample in the x and y directions in response to the current in the x direction, as integrals of the corresponding electrochemical potential gradients. We obtain

$$V_x = \frac{1}{e} \int_{-L_x/2}^{L_x/2} dx \frac{\partial \mu}{\partial x} = \frac{IL_x}{\sigma L_y^2} \left(1 - \frac{\lambda^2}{L_a^2} \cos^2 \theta \right) + \frac{2I \lambda^3 \cos^2 \theta}{\sigma L_y^2 L_a^2} \tanh(L_x/2\lambda), \quad (11)$$

and

$$V_y = \frac{1}{eL_x} \int_{-L_x/2}^{L_x/2} dx \int_{-L_y/2}^{L_y/2} dy \frac{\partial \mu}{\partial y} = -\frac{I \lambda^2 \cos \theta \sin \theta}{\sigma L_a^2 L_y} \left[1 - \frac{2\lambda}{L_x} \tanh(L_x/2\lambda) \right], \quad (12)$$

where we have averaged V_y along the length of the sample in the x direction.

Equations (11) and (12) then imply the following result for the scale-dependent resistivity tensor,

$$\begin{aligned}\rho_{xx} &= \frac{1}{\sigma} \left(1 - \frac{\lambda^2}{L_a^2} \cos^2 \theta \right) + \frac{2\lambda^2 \cos^2 \theta}{\sigma L_a^2 L_x} \tanh(L_x/2\lambda), \\ \rho_{yx} &= -\frac{\lambda^2 \sin \theta \cos \theta}{\sigma L_a^2} \left[1 - \frac{2\lambda}{L_x} \tanh(L_x/2\lambda) \right].\end{aligned}\quad (13)$$

The resistivity tensor thus contains both diagonal and off-diagonal components, the off-diagonal ones being induced by the magnetic field. Since λ is always dominated by the shortest of the two length scales $L_{a,c}$, it is clear that the off-diagonal resistivity vanishes when L_a diverges, making it clear that the origin of the off-diagonal component of the resistivity tensor is the chiral anomaly. More specifically, its origin can be easily traced back to the CME contribution to the electrical current in Eq. (2).

Equation (13) may be rewritten in a more illuminating form in terms of ρ_{\parallel} and ρ_{\perp} , i.e., diagonal components of the resistivity tensor, corresponding to the current flow along and perpendicular to the direction of the magnetic field. From Eq. (13), we have

$$\rho_{\parallel} = \frac{1}{\sigma} \left(1 - \frac{\lambda^2}{L_a^2} \right) + \frac{2\lambda^3}{\sigma L_a^2 L_x} \tanh(L_x/2\lambda), \quad \rho_{\perp} = \frac{1}{\sigma}.\quad (14)$$

Then Eq. (13) may be written as

$$\rho_{xx} = \rho_{\perp} - \Delta\rho \cos^2 \theta, \quad \rho_{yx} = -\Delta\rho \sin \theta \cos \theta, \quad (15)$$

where $\Delta\rho = \rho_{\perp} - \rho_{\parallel}$ is the chiral anomaly induced resistivity anisotropy.

Equation (15) has the form of a standard relation between the anisotropic magnetoresistance (AMR), represented by the first equation, and the planar Hall effect (PHE), which is expressed by the second equation [30–32]. Note that the name PHE is a bit of a misnomer: The off-diagonal resistivity does not satisfy the antisymmetry property of a true Hall effect $\rho_{xy} = -\rho_{yx}$, since it does not originate from the Lorentz force. It is, however, the standard name for this phenomenon in the literature and we will thus use it as well. Both AMR and PHE are well-known phenomena in ferromagnetic metals, originating in this case from the interplay of the magnetic order and the spin-orbit interactions. Both are typically very weak, but can be much stronger in ferromagnets with significant spin-orbit interactions, such as doped magnetic semiconductors [32]. What is remarkable about our result is that neither AMR nor PHE in a topological metal require magnetic order, originating instead from the chiral anomaly, and their magnitude can be extremely large (in fact, approaching the theoretical upper limit at increasing magnetic field), as we show below. The sign of the effect in our case is also opposite to what is typically observed in ferromagnets: $\Delta\rho$, as defined in Eq. (15), is positive in our case, but would typically be negative in a metallic ferromagnet [31].

The parallel resistivity ρ_{\parallel} exhibits a nontrivial dependence on the two intrinsic length scales $L_{a,c}$ of the material and on the sample size L_x . Let us first consider the regime of weak magnetic fields, corresponding to $L_a \gg L_c$. In this case, taking

the limit of large sample size $L_x \gg L_c$, we obtain

$$\rho_{\parallel} \approx \frac{1}{\sigma} \left[1 - \left(\frac{L_c}{L_a} \right)^2 \right], \quad (16)$$

which corresponds to a small negative quadratic magnetic-field-dependent correction to the longitudinal resistivity. The PHE in this case is also small and given by

$$\rho_{yx} = -\frac{1}{\sigma} \left(\frac{L_c}{L_a} \right)^2 \sin \theta \cos \theta. \quad (17)$$

A more interesting regime is the regime of stronger magnetic field, corresponding to $L_a \ll L_c$. Assuming the sample size $L_x > L_a$, we obtain

$$\rho_{\parallel} = \frac{L_a^2}{\sigma L_c^2} \left(1 + \frac{2L_c^2}{L_a L_x} \right). \quad (18)$$

Equation (18) exhibits an interesting and nontrivial scale dependence. Indeed, suppose that $L_a < L_x < L_c^2/L_a$ (the upper limit is a third nontrivial length scale in this problem). In this case,

$$\rho_{\parallel} \approx \frac{2L_a}{\sigma L_x} = \frac{4\pi^2 \ell_B^2}{e^2 L_x}. \quad (19)$$

To understand the meaning of this result, it is convenient to evaluate the corresponding conductance

$$G_{\parallel} = \frac{\rho_{\parallel} L_y}{L_x} = \frac{e^2 N_{\phi}}{2\pi}, \quad (20)$$

where $N_{\phi} = L_y^2/2\pi \ell_B^2$ is the number of magnetic flux quanta, penetrating the sample cross section. This is identical to the result of Ref. [29], obtained by a different method. Physically, this corresponds to a regime in which the sample conductance is dominated by the chiral lowest Landau level, which is where the chiral anomaly contribution to Eqs. (1) and (2) comes from [21,22]. G_{\parallel} then corresponds to a conductance of e^2/h per lowest Landau level orbital state, i.e., is identical to the conductance of an effective one-dimensional system with N_{ϕ} conduction channels.

Most importantly, the resistivity anisotropy and thus the magnitude of the PHE in this regime is given by

$$\Delta\rho = \frac{1}{\sigma} \left(1 - \frac{2L_a}{L_x} \right). \quad (21)$$

Thus $\Delta\rho$ is starting to approach its maximal possible value of $1/\sigma$ when the sample size is increased. We thus call this the giant planar Hall effect (GPHE) (this name was first used in relation to PHE in the context of magnetic semiconductors in Ref. [32]).

For larger sample sizes, when $L_x > L_c^2/L_a$, the magnetic field dependence of the longitudinal resistivity crosses over from $1/B$ to $1/B^2$,

$$\rho_{\parallel} \approx \frac{1}{\sigma} \left(\frac{L_a}{L_c} \right)^2. \quad (22)$$

The GPHE magnitude in this case becomes independent of the sample size and has reached its maximal magnitude,

$$\Delta\rho = \frac{1}{\sigma} \frac{(L_c/L_a)^2}{1 + (L_c/L_a)^2}, \quad (23)$$

which converges to $1/\sigma$ as the magnetic field is increased.

Interestingly, there exists a direct connection between the GPHE and the angular narrowing of the negative longitudinal magnetoconductivity signal [17], as we will now demonstrate. Using Eq. (15), we obtain

$$\begin{aligned}\rho_{xx}^{-1}(B) - \rho_{xx}^{-1}(0) &= \frac{\sigma(\Delta\rho/\rho_{\parallel})\cos^2\theta}{1 + (\Delta\rho/\rho_{\parallel})\sin^2\theta} \\ &= \frac{\sigma(L_c/L_a)^2\cos^2\theta}{1 + (L_c/L_a)^2\sin^2\theta}.\end{aligned}\quad (24)$$

What is missing in the standard expressions for the chiral anomaly induced magnetoconductivity [20] is the angular dependence in the denominator in Eq. (24). This clearly leads to narrowing of the angular dependence: Equation (24) at small angles has the form of a Lorentzian with the angular width $\Delta\theta \sim L_a/L_c$, which gets narrower as the magnitude of the chiral anomaly induced GPHE increases. This nontrivial connection between the GPHE and the angular narrowing of the negative longitudinal magnetoresistance signal may be regarded as a smoking gun evidence for the chiral anomaly.

In order to relate our results to the existing experimental data [17,18], it is useful to express the ratio L_c/L_a explicitly in terms of the magnetic field. We obtain

$$\frac{L_c}{L_a} = \Gamma B \sqrt{\frac{\tau_c}{D}} \sim \left(\frac{\hbar v_F/\ell_B}{\epsilon_F} \right)^2 \sqrt{\frac{\tau_c}{\tau}}, \quad (25)$$

where v_F is the Fermi velocity of the Weyl (Dirac) fermions, ϵ_F is the Fermi energy, and τ is the momentum relaxation time. Taking the values for these parameters from Ref. [17], we have $v_F \approx 3.5 \times 10^7$ cm/s, $\epsilon_F \approx 30$ meV, and $\tau_c/\tau \approx 50$. Assuming the density of states to be $g = \epsilon_F^2/2\pi^2\hbar^3 v_F^3$, and substituting the above values in Eq. (25), we obtain $L_c/L_a \approx 0.7B/1$ T.

In Fig. 2 we plot both the angular dependence of the inverse longitudinal magnetoresistivity and the magnitude of the GPHE using L_c/L_a values, which correspond to the range of magnetic fields of up to about 10 T, which was used in Refs. [17,18]. Qualitatively, the behavior of the magnetoresistivity appears to agree with the experimental data. In particular, at low magnetic fields, the magnetoconductivity peak follows a B^2 dependence, while the angular width goes roughly as $1/B$, consistent with Eqs. (24) and (25). At higher fields both appear to saturate, which is likely explained by the fact that in both experiments the quantum regime $\epsilon_F < \hbar v_F/\ell_B$ is reached at magnetic fields of just a few T. In this regime, we expect $g \sim B$ and $1/\tau \sim B$, $1/\tau_c \sim B$, thus making the ratio L_c/L_a independent of the magnetic field. Figure 2 also shows that the magnitude of the GPHE may approach its maximal value of $\Delta\rho = 1/\sigma$ for experimentally accessible values of the magnetic field.

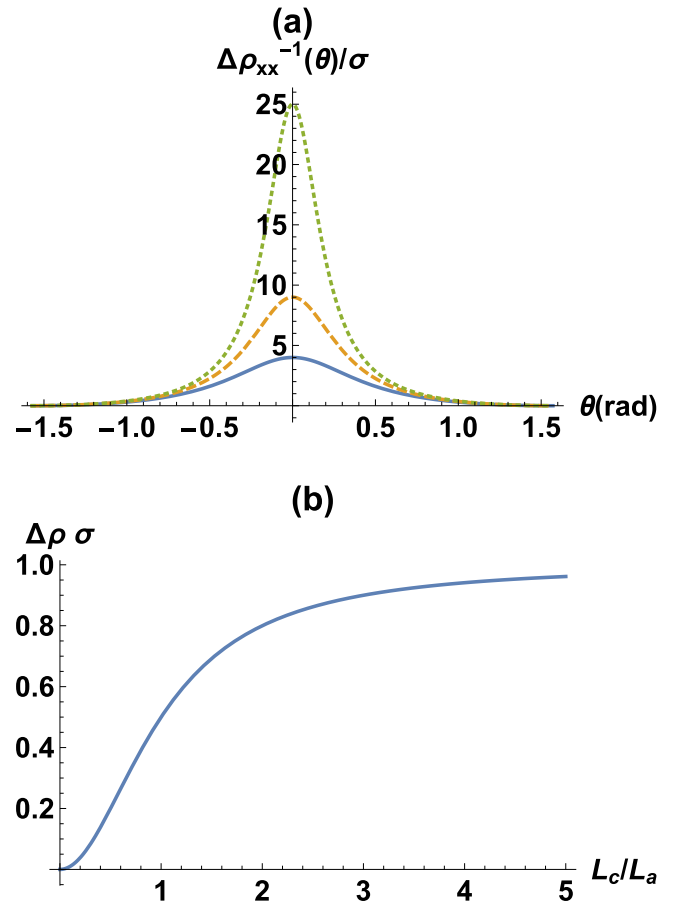


FIG. 2. (a) Inverse longitudinal magnetoresistivity as a function of the angle between the current and the magnetic field. Different curves correspond to different values of the ratio L_c/L_a : 2 (blue, solid), 3 (orange, dashed), and 5 (green, dotted). (b) Dependence of the resistivity anisotropy $\Delta\rho$ and thus the magnitude of the GPHE on L_c/L_a .

In conclusion, we have described a magnetotransport effect, related to the chiral anomaly, called the giant planar Hall effect. We have also connected this effect to the angular dependence of the longitudinal magnetoconductivity, explaining its magnetic-field-dependent narrowing, pointed out in Ref. [17]. Observation of both the negative longitudinal magnetoresistance and the GPHE, with a specific relation between the angular dependence of the magnetoresistance and the GPHE magnitude, given by Eq. (24), constitutes a smoking gun evidence for the chiral anomaly. We note that the GPHE may have already been observed in a recent experiment on ZrTe₅ [33].

We acknowledge useful discussions with Nai Phuan Ong. Financial support was provided by Natural Sciences and Engineering Research Council (NSERC) of Canada.

[1] X. Wan, A. M. Turner, A. Vishwanath, and S. Y. Savrasov, *Phys. Rev. B* **83**, 205101 (2011).

[2] K.-Y. Yang, Y.-M. Lu, and Y. Ran, *Phys. Rev. B* **84**, 075129 (2011).

- [3] A. A. Burkov and L. Balents, *Phys. Rev. Lett.* **107**, 127205 (2011).
- [4] A. A. Burkov, M. D. Hook, and L. Balents, *Phys. Rev. B* **84**, 235126 (2011).
- [5] G. Xu, H. Weng, Z. Wang, X. Dai, and Z. Fang, *Phys. Rev. Lett.* **107**, 186806 (2011).
- [6] S. M. Young, S. Zaheer, J. C. Y. Teo, C. L. Kane, E. J. Mele, and A. M. Rappe, *Phys. Rev. Lett.* **108**, 140405 (2012).
- [7] Z. Wang, Y. Sun, X.-Q. Chen, C. Franchini, G. Xu, H. Weng, X. Dai, and Z. Fang, *Phys. Rev. B* **85**, 195320 (2012).
- [8] Z. Wang, H. Weng, Q. Wu, X. Dai, and Z. Fang, *Phys. Rev. B* **88**, 125427 (2013).
- [9] Z. K. Liu, B. Zhou, Y. Zhang, Z. J. Wang, H. M. Weng, D. Prabhakaran, S.-K. Mo, Z. X. Shen, Z. Fang, X. Dai, Z. Hussain, and Y. L. Chen, *Science* **343**, 864 (2014).
- [10] M. Neupane, S.-Y. Xu, R. Sankar, N. Alidoust, G. Bian, C. Liu, I. Belopolski, T.-R. Chang, H.-T. Jeng, H. Lin, A. Bansil, F. Chou, and M. Z. Hasan, *Nat. Commun.* **5**, 3786 (2014).
- [11] S.-Y. Xu, I. Belopolski, N. Alidoust, M. Neupane, G. Bian, C. Zhang, R. Sankar, G. Chang, Z. Yuan, C.-C. Lee, S.-M. Huang, H. Zheng, J. Ma, D. S. Sanchez, B. Wang, A. Bansil, F. Chou, P. P. Shibayev, H. Lin, S. Jia, and M. Z. Hasan, *Science* **349**, 613 (2015).
- [12] B. Q. Lv, N. Xu, H. M. Weng, J. Z. Ma, P. Richard, X. C. Huang, L. X. Zhao, G. F. Chen, C. E. Matt, F. Bisti, V. N. Strocov, J. Mesot, Z. Fang, X. Dai, T. Qian, M. Shi, and H. Ding, *Nat. Phys.* **11**, 724 (2015).
- [13] B. Q. Lv, H. M. Weng, B. B. Fu, X. P. Wang, H. Miao, J. Ma, P. Richard, X. C. Huang, L. X. Zhao, G. F. Chen, Z. Fang, X. Dai, T. Qian, and H. Ding, *Phys. Rev. X* **5**, 031013 (2015).
- [14] L. Lu, Z. Wang, D. Ye, L. Ran, L. Fu, J. D. Joannopoulos, and M. Soljačić, *Science* **349**, 622 (2015).
- [15] S. L. Adler, *Phys. Rev.* **177**, 2426 (1969).
- [16] J. S. Bell and R. Jackiw, *Nuovo Cimento A* **60**, 4 (1969).
- [17] J. Xiong, S. K. Kushwaha, T. Liang, J. W. Krizan, M. Hirschberger, W. Wang, R. J. Cava, and N. P. Ong, *Science* **350**, 413 (2015).
- [18] Q. Li, D. E. Kharzeev, C. Zhang, Y. Huang, I. Pletikoscic, A. V. Fedorov, R. D. Zhong, J. A. Schneeloch, G. D. Gu, and T. Valla, *Nat. Phys.* **12**, 550 (2016).
- [19] M. Hirschberger, S. Kushwaha, Z. Wang, Q. Gibson, S. Liang, C. A. Belvin, B. A. Bernevig, R. J. Cava, and N. P. Ong, *Nat. Mater.* **15**, 1161 (2016).
- [20] D. T. Son and B. Z. Spivak, *Phys. Rev. B* **88**, 104412 (2013).
- [21] A. A. Burkov, *Phys. Rev. Lett.* **113**, 247203 (2014).
- [22] A. A. Burkov, *Phys. Rev. B* **91**, 245157 (2015).
- [23] A. A. Burkov and Y. B. Kim, *Phys. Rev. Lett.* **117**, 136602 (2016).
- [24] S. A. Parameswaran, T. Grover, D. A. Abanin, D. A. Pesin, and A. Vishwanath, *Phys. Rev. X* **4**, 031035 (2014).
- [25] A. A. Zyuzin, S. Wu, and A. A. Burkov, *Phys. Rev. B* **85**, 165110 (2012).
- [26] K. Fukushima, D. E. Kharzeev, and H. J. Warringa, *Phys. Rev. D* **78**, 074033 (2008).
- [27] M. M. Vazifeh and M. Franz, *Phys. Rev. Lett.* **111**, 027201 (2013).
- [28] Y. Chen, S. Wu, and A. A. Burkov, *Phys. Rev. B* **88**, 125105 (2013).
- [29] A. Altland and D. Bagrets, *Phys. Rev. B* **93**, 075113 (2016).
- [30] J. P. Pan, in *Solid State Physics*, edited by F. Seitz and D. Turnbull (Academic, New York, 1957), Vol. 5, pp. 1–96.
- [31] K. Hong and N. Giordano, *Phys. Rev. B* **51**, 9855 (1995).
- [32] H. X. Tang, R. K. Kawakami, D. D. Awschalom, and M. L. Roukes, *Phys. Rev. Lett.* **90**, 107201 (2003).
- [33] T. Liang, Q. Gibson, M. Liu, W. Wang, R. J. Cava, and N. P. Ong, [arXiv:1612.06972](https://arxiv.org/abs/1612.06972).